Int J Adv Manuf Technol (2016) 86:1393–1405
DOI 10.1007/s00170-015-8245-1

ORIGINAL ARTICLE

Influence of microstructure and hardness on machinability of heat-treated titanium alloy Ti-6Al-4V in end milling with polycrystalline diamond tools

Sarwar Ali Abbasi [1] · Pingfa Feng [1] · Yuan Ma [1] · Jianfu Zhang [1] · Dingwen Yu [1] · Zhijun Wu [1]

Received: 2 June 2015 / Accepted: 15 December 2015 / Published online: 9 January 2016

Abstract The main objective of this paper is to develop the relationship between microstructure and machinability of titanium alloy Ti-6Al-4V which is given heat treatment beyond β transus temperature, with the help of milling experiments using polycrystalline diamond (PCD) tools. Two of the specimens were solution treated at 1050 °C/1 h. After the treatment, one of the specimen was cooled in water while the other specimen was air-cooled, followed by aging treatment at 550 °C/4 h. The third specimen was used in as-received condition (casted). Cutting speed, feed rate, and depth of cut were varied, and their effects have been analyzed on cutting forces, vibration amplitude, temperature, and tool wear for all the three specimens. The results have shown improved and better machinability for the specimen which was cooled in air after the solution treatment with PCD tools. This behavior of the alloy is mainly attributed to formation of homogeneous lamellar $\alpha+\beta$ Ti-6Al-4V microstructure. Although, the air-cooled specimen has higher hardness than the as-received specimen. But, the former alloy's fine homogeneous and lamellar $\alpha+\beta$ Ti-6Al-4V microstructure as compared to the microstructure of the latter specimen (irregular $\alpha+\beta$ Ti-6Al-4V structure) and absence of α' secondary precipitate (found in water-cooled specimen) has helped in giving improved performance. Thus, from this study, it can be concluded that machinability of titanium alloy Ti-6Al-4V can be further improved with controlled heat treatment process using PCD tools.

Keywords Heat-treated titanium alloys · Polycrystalline diamond inserts · Machinability · Vibration · Cutting forces · Tool wear

✉ Pingfa Feng
fengpf@tsinghua.edu.cn

Sarwar Ali Abbasi
abbasisa10@mails.tsinghua.edu.cn

Yuan Ma
yuan-ma11@mails.tsinghua.edu.cn

Jianfu Zhang
zhjf@mail.tsinghua.edu.cn

Dingwen Yu
yudw@tsinghua.edu.cn

Zhijun Wu
wuzhijun@tsinghua.edu.cn

[1] State Key Laboratory of Tribology, Department of Mechanical Engineering, Tsinghua University, Haidain District, Beijing 100084, People's Republic of China

1 Introduction

Due to poor machinability of titanium alloy Ti-6Al-4V [1–3], new titanium alloys are being developed having better strength and machinability. However, Ti-6Al-4V is still widely used in the aerospace industry. Many researchers are trying to apply different innovative techniques like different heat treatment cycles, cutting tool material, and cutting processes in order to improve its machinability. Some of these methodologies are discussed here:

Carbide base tool materials are most often employed for the machining of titanium alloys because of their low cost and availability in almost any form. But usually very low cutting speeds are employed to avoid rapid wear of cutting tool because of their low hot strength and poor thermal conductivity. In the literature, some authors [3–5] have investigated the effect of various coating layers on machinability of Ti-6Al-4V by studying tool wear, vibration, thermal characteristics, cutting forces, and surface roughness concluding that no considerable improvement in machinability is obtained with this approach. This has ultimately resulted in the use of super hard cutting tool materials. Among various super hard cutting tool materials, polycrystalline diamond (PCD) tool has shown significant improvement in machinability, tool life, and surface quality as reported in literature [6–13]. However in these studies, parameters like microstructure and hardness of alloy have not been considered which also have great effect on machinability. Although, there are a number of studies where authors have investigated the effect of microstructure and hardness on the machinability of titanium alloys. In most of the cases, titanium alloy Ti-6Al-4V has been used in annealed or in as-received conditions and its machinability has been compared with other heat-treated titanium alloys with carbide tools. Some of these are explained below in detail:

Kosaka and Fox (2004) and Kosaka et al. [14, 15] investigated the machinability of Ti-6Al-4V in as-received condition and compared the results with other titanium alloy Ti54M in different heat-treated conditions and found that machinability of Ti54M is better than Ti-6Al-4V because of better microstructure of former alloy. Khana et al. [16] evaluated the machinability of Ti54M alloy in different heat-treated conditions and compared the results with Ti-6Al-4V in annealed condition by varying cutting speed and feed rate. The authors concluded that Ti54M alloy has the highest cutting forces in the aged condition due to high hardness, whereas in annealed or in as-received condition machinability of Ti54M is better than Ti-6Al-4V because of better microstructure of Ti54M alloy. Similar experiments were carried out by Khana and Sangwan [17], where they used $\alpha+\beta$ alloy Ti54M and β alloy Ti 10-2-3 and investigated the machinability of two alloys in as-received condition and compared the results when the two alloys were used in annealed and in solution-treated-plus-aged condition. Cutting speed and feed rate was varied and their effects on cutting forces and temperature were observed. From the study, it was found that in solution-treated-plus-aged condition, both alloys showed poor machinability while in annealed and in as-received condition, Ti54M alloy showed superior machinability due to its better microstructure. Rahim et al. [18] compared the performance of two titanium alloys, namely Ti54M and Ti-6Al-4V, in drilling with carbide tool at lower cutting speeds. From their research, authors found that the tool used in drilling for Ti-6Al-4V has higher tool life. Vanktesh et al. [19] analyzed the machinability of two titanium alloys vis-à-vis Ti54M and Ti-6Al-4 V from low cutting speed to higher cutting speed in orthogonal turning process with carbide tools. Authors concluded that at higher cutting speed, the machinability of Ti54M is better than Ti-6Al-4V. Armendia et al. [20] in their research work concluded that due to better microstructure of Ti54M alloy, its machinability is better than Ti-6Al-4V. Azam et al. [21] studied the effect of microstructure of high-strength low alloy steel grade on surface roughness in turning with varying cutting parameters and developed the prediction model using ANOVA analysis. The authors concluded that machinability is greatly affected by heat treatment process.

The abovementioned studies suggest that machinability greatly depends on the work material microstructure which in turn greatly depends on the heat treatment process. The machinability of Ti54M was concluded better than Ti-6Al-4V in as-received or annealed condition due to better microstructure of former alloy. On the other hand, in solution-treated-plus-aged condition (below β transus temperature) poor machinability was exhibited by all the titanium alloys with carbide tools due to their increased strengthening effect. Furthermore, the case studies in literature studying the effect of cutting tool material on machinability of titanium alloy Ti-6Al-4V in as-received condition have shown dominance of PCD tools. Since PCD tool has higher hot strength, higher thermal conductivity, and low wear rate, therefore, it is necessary to testify its effectiveness on machinability of titanium alloy Ti-6Al-4V in different heat-treated conditions. Moreover, in most of the published literature where heat treatment effect has been investigated, the solution treatment of alloys has been carried out well below the β transus temperature.

Thus, there is a need to explore machinability of heat-treated titanium alloy Ti-6Al-4V with PCD tools beyond β transus temperature which can have a strong effect on alloy's microstructure and ultimately affecting its machinability. The objective of the research, variables studied and parameters to be investigated are highlighted in Fig. 1.

2 Experimental plan and setup

To study the effectiveness of PCD tool on machinability of heat-treated titanium alloy, elaborate experiments were performed on titanium alloy Ti-6Al-4V in as-received and two different heat-treated conditions. The details on experimental setup, workpiece specifications, cutting tool specifications, and cutting parameters are discussed in the following sections:

2.1 Machining setup details

Experiments were performed on five-axes high-speed vertical machining center, DMU60 Mono Block having max. rpm of 18,000 and spindle taper of HSK 63A, which is a dynamically balanced spindle system. A typical experimental setup is shown in Fig. 2.

A workpiece was clamped on a three-directional force measuring equipment, Dynamometer (Kistler 5070) through specially designed fixture for measuring cutting forces. Two three-directional accelerometers were mounted on the workpiece and a machine spindle, as shown in Fig. 2, to record the vibration signals during machining, and the signals were

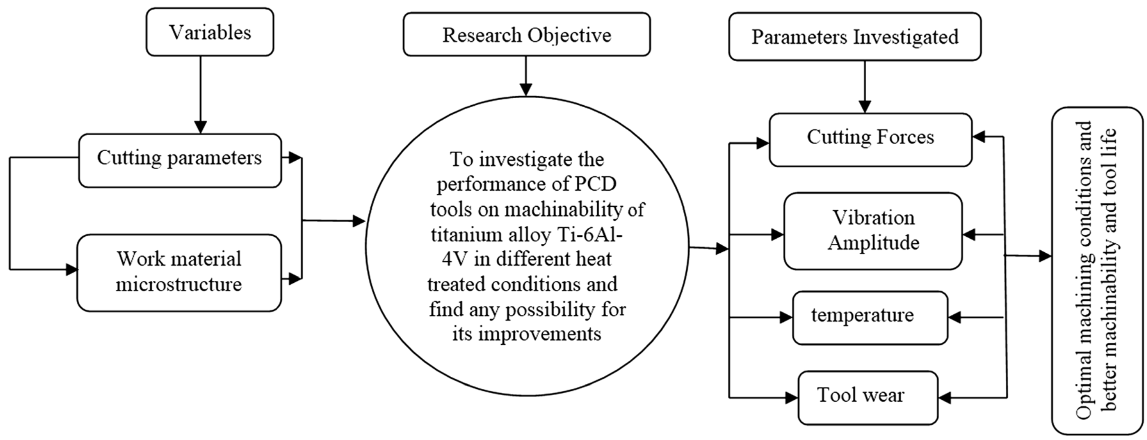

Fig. 1 Complete research layout

analyzed on a dynamic cutting software, LMS. A thermal imaging camera R300 InfRec infrared camera was used for measuring the average cutting temperature of the cutting zone. A toolmaker microscope and a scanning electron microscope (SEM) were used to study the wear mechanism of the inserts used in the experiments.

2.2 Workpiece specifications

To study the effect of microstructure and hardness of Ti-6Al-4V on its machinability, workpieces in rectangular shape of size 35 × 25 × 80 mm received in cast conditions were heat treated at two different conditions. The two specimens were solution treated at 1050 °C/1 h followed by aging at 550 °C/4 h. One of the heat-treated specimen was allowed to cool in air after solution treatment while the other was cooled in water and the third workpiece was used in as-received condition to obtain different microstructures and hardness. The hardness values of all three specimens were recorded by Tukon 2500-6 Knoop/Vickers automated hardness tester. For as-received sample (alloy-A), it was measured as 320~345 HV; 365~390 HV for the heat-treated-air-cooled sample (alloy-B), and 410~430HV for the heat-treated-water-cooled specimen (alloy-C).

The microstructure of all three specimens was analyzed using SEM as shown in Fig. 3. Fine lamellar $\alpha + \beta$ structure has been obtained for the alloy-B, which is attributed to a slow cooling rate of the air as shown in Fig. 3b. Figure 3a shows the microstructure of alloy-A. It has two phases α and β solution in which α phase has a coarse lamellar structure mutually connected in basket weave form and in between thin β phase lies. The microstructure of the alloy-C is shown in Fig. 3c, the specimen has acicular α' martensite phase, formed due to rapid cooling in water [22].

2.3 Cutting tool details

Two fluted end mill of diameter 16 mm was used in all the experiments. A PCD insert brazed on carbide substrate having a nose radius of 0.4 mm, clearance angle of 11°,

Fig. 2 Experimental setup

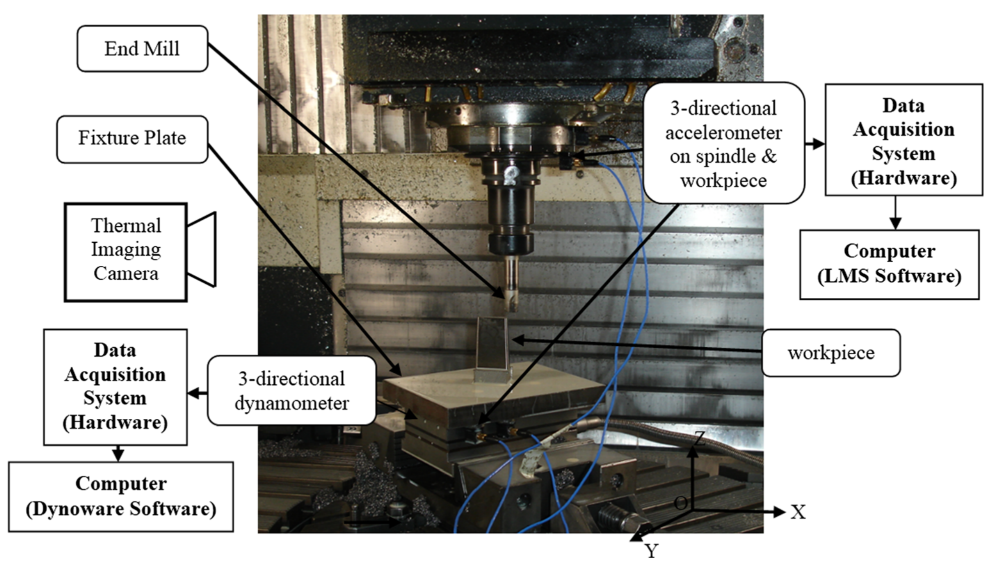

Fig. 3 Titanium alloy Ti-6Al-4V microstructure

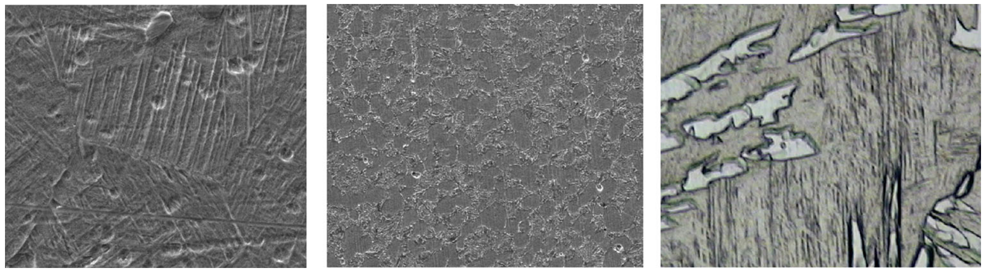

a) As-received alloy b) STA alloy cooled in air c) STA alloy cooled in water

radial rake angle of 15°, and axial rake angle of 0° was used in all the experiments.

2.4 Details on machining parameters

Cutting parameters, namely, cutting speed, feed per tooth, and axial depth of cut were varied and their effect on cutting forces, vibration, temperature, and tool wear for all three Ti-6Al-4V alloy specimens have been studied. Up milling strategy was used in all the experiments. Each experiment was run for an average of 5 min. For every experiment, a new insert was used and each experiment was repeated twice in order to minimize the uncertainties in the measurements. The average value of the maximum values recorded during each experiment was used for further analysis. The radial engagement of tool was kept constant at 2 mm for all the experiments. Five levels of each variable have been used in the experiments in order to study in detail the effect of each parameter by varying only one parameter at a time and other two being constant. First five experiments show the level of cutting speed used in the experiments where axial depth of cut and feed per tooth were kept constant. Then, the next five experiments show the level of feed per tooth used to analyze its effect at a constant cutting speed and axial depth of cut. Similarly, in the last five experiments, only the axial depth of cut was varied to study its effect only. The parameters are shown in Table 1.

3 Results and discussion

Experimental results for cutting forces, vibration, temperature, and tool wear for three different titanium alloy Ti-6Al-4V specimens are discussed here.

3.1 Analysis of cutting forces

Cutting force is an important machinability evaluation parameter as it can predict how long the tool will work efficiently and provide good surface quality. According to Anayet et al. [23], cutting forces are greatly influenced by the cutting parameters. Therefore, it is important to study the behavior of three Ti-6Al-4V specimens (alloy-A, alloy-B, and alloy-C) at various cutting parameters in order to find optimal cutting conditions. Cutting forces were recorded for all the experiments with dynamometer (Kistler 5070). For the analysis, the main cutting force, calculated from the average measured forces of feeding directional (F_X) and tangential directional (F_Y) forces, has been selected and results are plotted in Fig. 4. The plotted results show the average values taken of the maximum forces recorded during each experiment with standard deviation of ±12 N.

It has been observed that cutting force values are in relationship with alloy microstructure and then with hardness. Lower values are obtained for alloy-B attributed mainly to fine regular lamellar $\alpha+\beta$ Ti-6Al-4V microstructure. Although hardness values of alloy-B are slightly higher than the hardness of alloy-A, coarse lamellar α structure of alloy-A compared to fine regular lamellar $\alpha+\beta$ Ti-6Al-4V microstructure mainly results in higher forces. For alloy-C, the highest forces have been observed at all the conditions

Table 1 Details on cutting parameters used in the experiments

Experiment no.	Cutting speed, V_C (m/min)	Feed per tooth, f_z (mm/tooth)	Axial depth of cut, a_p(mm)	Material removal rate (mm^3/min)
1.	100			800
2.	120			955
3.	150	0.10	1.0	1194.26
4.	170			1353.5
5.	200			1592.35
6.		0.05		597.1
7.		0.07		836
8.	150	0.10	1.0	1194.26
9.		0.12		1433.12
10.		0.15		1791.4
11.			0.2	238.85
12.			0.5	597.13
13.	150	0.10	1.0	1194.26
14.			1.2	1433.12
15.			1.5	1791.4

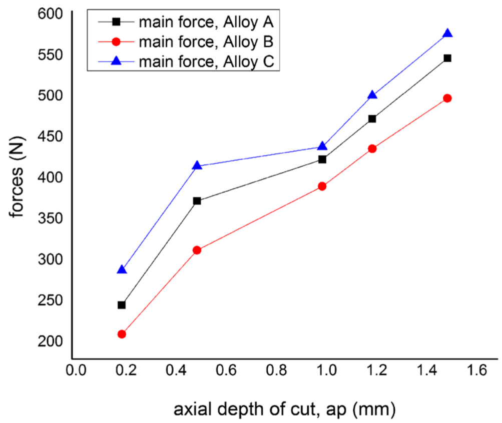

(a) effect of axial depth of cut

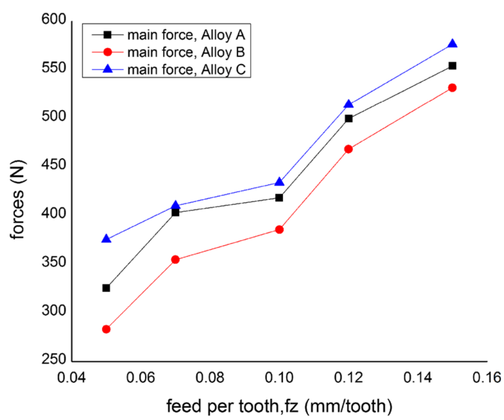

(b) effect of feed per tooth

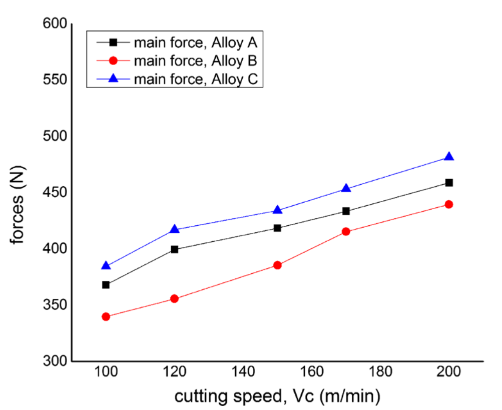

(c) effect of cutting speed

Fig. 4 Main cutting force for three different Ti-6Al-4V specimens at various cutting conditions

studied. The main reason for such behavior of the alloy seems to be the presence of α' martensite phase in microstructure along with the highest value of hardness. The coarse microstructure during machining requires higher shear energy to remove the metal and results in higher forces. The formation of α' martensite phase due to a fast cooling rate of water, interference with dislocation of α particles and increased strengthening effect along with the higher hardness are the main causes for higher forces of alloy-C. The results depict that performance of PCD tool is more dependent on the microstructure of the alloy as lower values are achieved for the alloy having better microstructure (alloy-B). Therefore, if better microstructure could be achieved through a controlled heat treatment process, then moderate increase in hardness value can be compensated with higher thermal conductivity and higher hot strength of PCD tool which could not be possible with carbide tools [16, 17] where the alloy with higher hardness has poor machinability irrespective of its microstructure.

Results also show that cutting forces are strongly influenced by increase in axial depth of cut and feed per tooth. Cutting forces rise to great extent with the increase in axial depth of cut and feed rate with more strong influence of axial depth of cut than feed per tooth. Slight or moderate increase in cutting force values has been observed with increase in cutting speed once cutting speed used in excess of 150 m/min. The main reason for such a phenomenon is related to couple effect of increased feed rate and rotational speed which when combined with higher axial depth of cut and feed per tooth results in such behavior. Similar results were also achieved in experimental work of [9] where a higher vibration amplitude was observed at higher cutting speed even though feed per tooth and axial depth of cut were constant. The higher depth of cut and feed rate at higher cutting speeds creates extra load on the cutting edge, thus causing increase in the shear energy and moderate increase in cutting forces.

3.2 Analysis of vibration on spindle and workpiece

Vibrations during machining greatly affect the tool life, surface quality of the component being machined, and also the life of the machine tool spindle itself. Therefore, it is important to study the behavior of the alloy's microstructure and hardness on vibrations produced during machining with PCD tool. Vibration amplitude was measured during experimentation for the spindle and workpiece with three-directional accelerometers mounted on the spindle and workpiece. The average values of maximum vibration amplitudes occuring in feeding (X-direction) and tangential (Y-direction) directions measured during experimentation for each test are used for further analysis, and the results are plotted in Fig. 5. The max. standard deviation for each average result is within ±0.18 g.

The plots of vibration amplitude in feeding and tangential cutting direction represent the average values of maximum vibration amplitudes recorded during each experimentation every time with a new insert. Results obtained for the vibration amplitude as shown in Fig. 5 above are in compliance with those obtained for the cutting forces, i.e., alloy's microstructure and hardness have key influence on the vibrations amplitude as well. Figure 5 shows the vibration values

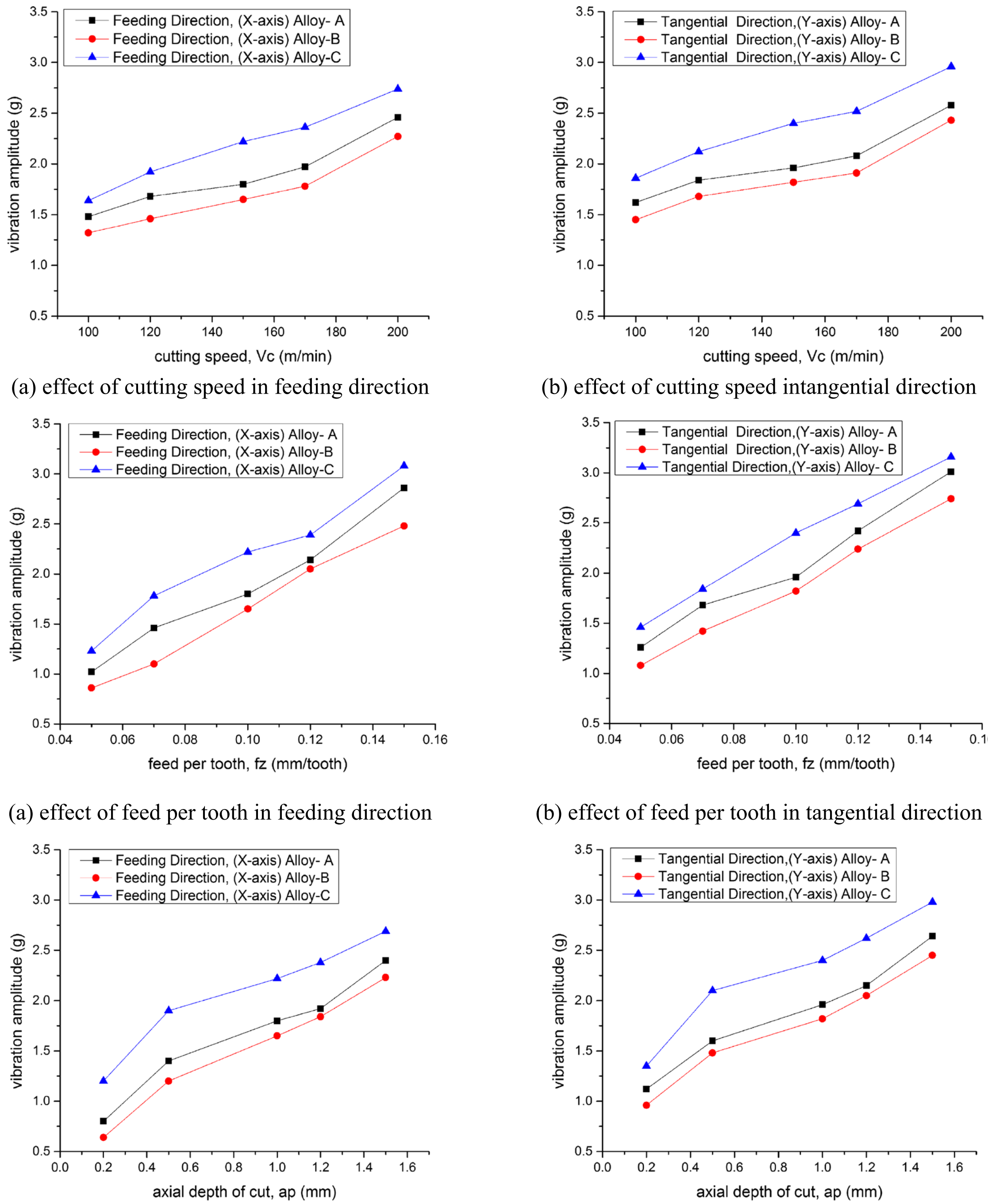

(a) effect of cutting speed in feeding direction (b) effect of cutting speed intangential direction

(a) effect of feed per tooth in feeding direction (b) effect of feed per tooth in tangential direction

(a) effect of axial depth of cutin feeding direction (b) effect of axial depth of cutin tangential direction

Fig. 5 Vibration amplitude in feeding and tangential cutting direction

measured through the accelerometer mounted on the spindle surface, whereas the vibration amplitude was also measured on the workpiece surface through the accelerometer mounted on the fixture plate but those results are not shown here because of two reasons. Firstly, vibration amplitude measured was quite low as compared to vibration amplitude measured through the accelerometer mounted on the spindle and secondly, in most of the cases, a similar trend as shown in Fig. 5 was observed. The results have shown PCD insert superiority for alloy-B inspite of moderate increase in hardness. This behavior is mainly attributed to homogeneous lamellar $\alpha + \beta$ formed due to β-annealing (solution treatment beyond β transus temperature, followed by air cooling). With this microstructure, the amount of shear energy required for removing material is evenly distributed over the cutting edge, thus resulting in better machinability results. The higher strength

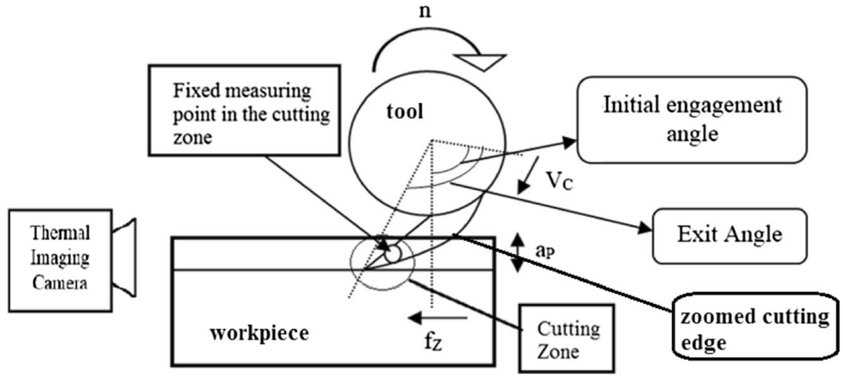

Fig. 6 Illustration of temperature measurement through thermal imaging camera

and thermal conductivity of PCD tool is another reason of superior performance for β-annealed alloy. Results have shown that vibration amplitude increases more rapidly once the higher cutting speed is used in combination of higher feed rate and depth of cut. Higher influence is seen for axial depth of cut and feed per tooth in terms of vibration amplitude, and moderate or low increase has been seen for the cutting speed. For cutting speed initially when varied from 100 to 150 m/min, there is very low increase in vibration amplitude but once cutting speed is used in excess of 170 m/min, higher increase has been observed which shows that at higher cutting speed, PCD tool also vibrates at higher amplitude; but with the alloy having better microstructure, this phenomenon seems to be in well-acceptable limits (amplitude of 2.1 g for alloy-B as compared to 2.3 g for alloy-A and 2.8 g for alloy-C). The increase with cutting speed at constant feed per tooth and axial depth of cut is mainly attributed to the use of higher depth of cut and feed rate, and when the combination of these high cutting parameters combines with a higher cutting speed, the insert experiences more load to remove the material and hence vibrates at higher amplitude. Similar observations have been also reported in the research work of [24].

3.3 Analysis of temperature

The energy required to convert the metal into chips is mostly converted into heat. This heat is transferred through conduction to chip, cutting tool, workpiece, and cutting fluid. The amount of heat transferred to chip, cutting tool, workpiece, and cutting fluid depends upon the physical and chemical properties of cutting tool, cutting fluid, workpiece material, and cutting conditions being employed. The cutting temperature on tool edge is also an important machinability evaluation parameter as higher temperature can cause rapid wear of the cutting tool and can also result in poor surface quality. Therefore, it is important to know the temperature in the cutting zone. However, in the milling process, due to rotary movement of the tool, temperature is continuously changing on the tool edge and it is not possible to accurately measure the cutting temperature at the tool edge representing the actual heat generated in the shear zone. Despite this fact, it is still important to establish a relationship between the alloy's microstructure and cutting parameters with temperature, even though this temperature may not be the exact temperature and will only represent an average temperature of the cutting zone due to disturbances that occurred in the milling process.

To study the thermal behavior of the three different titanium alloy Ti-6Al-4V specimens at various cutting conditions, temperature in the cutting zone has been measured using thermal imaging camera R300 InfRec infrared camera. The use of a thermal imager for measurement of temperature in the cutting zone is quite known among the research community. It can be used to measure the temperature in the range of −40 to 2000 °C with an accuracy of ±2 %, sensitivity and spatial

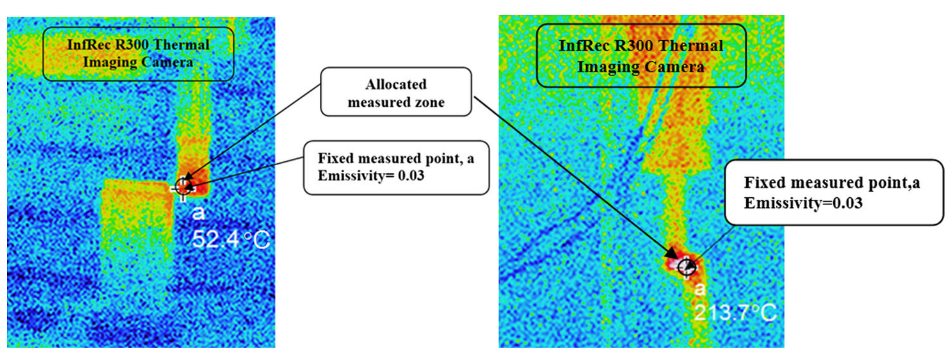

(a) thermal image before cutting (b) thermal image during cutting, exp#5

Fig. 7 Thermal images with InfRec R300 thermal imaging camera and analyzing results in InfRec NS9500 Standard Analyzer

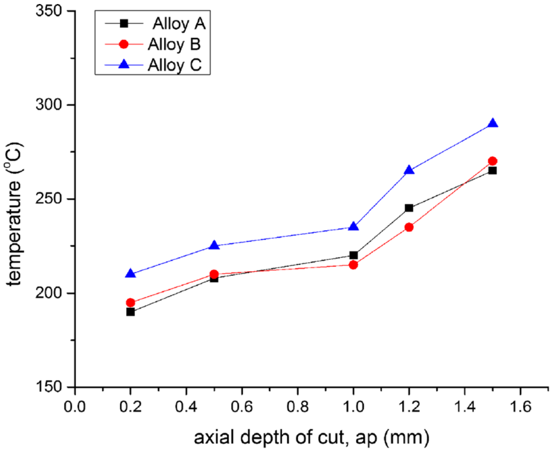

(a) effect of axial depth of cut,a_P

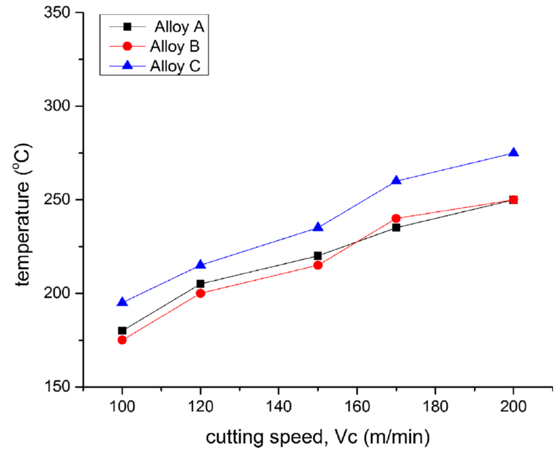

(b) effect of cutting speed, V_C

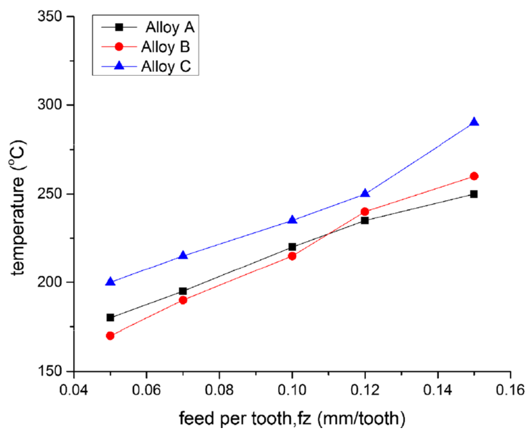

(c) effect of feed per tooth, f_Z

Fig. 8 Average temperature at various cutting conditions for three Ti-6Al-4V specimens

resolution of 0.05 °C and can take image at a frame rate of 760 Hz with InfRec Analyzer NS9500 Standard package. The experimental setup to measure the temperature is shown in Fig. 2. A fixed point near the cutting edge in the cutting zone, as shown in Fig. 6 which could represent the average cutting temperature in the cutting zone, is selected for measurement. Several readings were taken during each experiment, and for every experiment, the reading representing the true cutting edge temperature involved in cutting is further selected for the analysis. To assure the measurement accuracy during experimentation, it has been tried to keep the same measuring time during each cycle so that the measured point in the cutting zone could be at the same distance in the cutting zone. The infrared image of static milling system during experimentation and before cutting is shown in Fig. 7 and shows the temperature measured on the fixed point in the cutting zone representing the average temperature of the cutting zone. Emissivity which has an important role in determining actual

Fig. 9 Wear of PCD tool for three work specimens after test #05

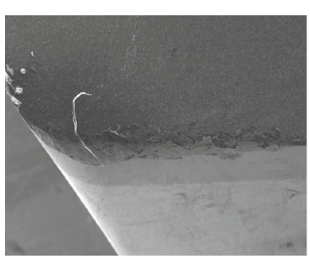

(a) Wear of alloy-A

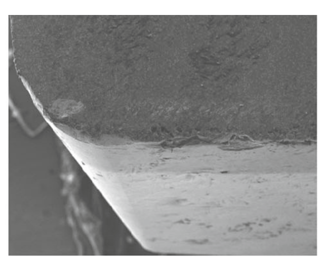

(b) wear of alloy-B

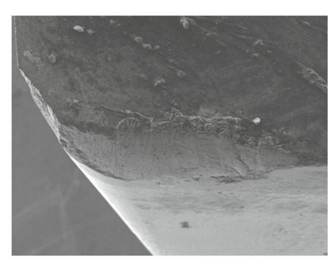

(c) wear of alloy-c

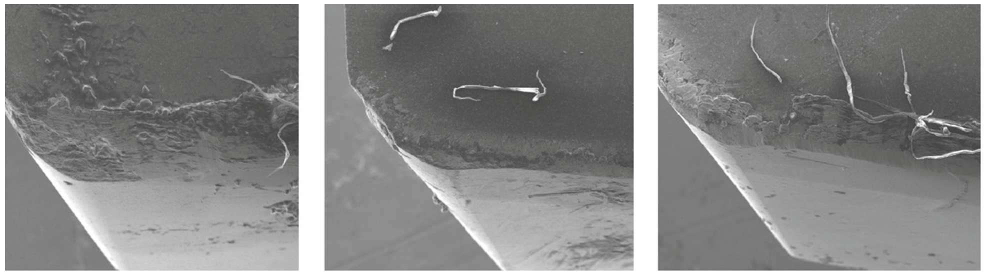

(a) wear of alloy-A (b) wear of alloy-B (c) wear of alloy-c

Fig. 10 Wear of PCD tool for three work specimens after test #10

temperature in the cutting zone was known by matching the temperature with a known temperature, and average emissivity value used in the temperature measurement for PCD tool was around 0.03.

The average temperature values measured during each experiment for the three Ti-6Al-4V specimens are shown in Fig. 8. The max. error bar calculated for each measurement is well within ±13 °C.

Results plotted for temperature analysis, as shown in Fig. 8, represent the temperature measured in the cutting zone at a fixed point which can depict the average temperature of the tool rake face. The Fig. 8 shows that with the increase in cutting speed, feed rate, and depth of cut, the tendency in heat generation also increases, which is mainly due to increase in shearing energy, increase in the contact area in the cutting zone, and increase in the friction due to increase in the interface between the tool forward-facing cutting plane and workpiece. The results show that due to higher thermal conductivity of PCD insert, a very low temperature has been measured for all three specimens at every cutting condition studied as compared to the carbide tools [16, 17]. However, an unclear difference in the results of temperature measurement for alloy-A and alloy-B has been observed, in contrast to considerable difference reported for the two alloys in the results of cutting forces and vibration amplitude (Section 3.1 and 3.2). The reason for this phenomenon could be due to the error in thermal measurements with thermal imaging camera which can occur because of decrease in elastic modulus of elasticity at higher temperatures [25]. Fluctuation in tool-chip interface due to rotary movement of the cutting tool is also another possible cause for this uncertainty in the thermal measurement system. However, a higher temperature has been measured for the alloy-C at all the cutting conditions, though the difference is not as high as in cutting forces and vibration amplitude results, arguably due to the abovementioned possible errors in the temperature measurement system. It has been observed that at combination of higher cutting speed, feed rate, and depth of cut, the higher temperature has been measured for alloy-C, and the difference with other two alloys is also quite significant. This shows that increased hardness and strengthening effects of alloy-C as compared to the other two alloys and the presence of α' martensite phase in its microstructure cause interference with dislocations of α particles and thus create a higher rubbing effect and produce higher friction during cutting and ultimately result in higher heat generation. This phenomenon becomes dominant enough at higher cutting conditions to be captured through infrared camera.

3.4 Tool wear mechanism analysis

Tool wear for all the inserts used in experiments has been analyzed with optical microscope and SEM, while wear land has been measured with the ToupTek microscope software. EDAX analysis of the worn cutting edge has been carried out to study the type of chemical reactions that occurred on the cutting edge for the inserts used on all three types of work specimens.

Figures 9, 10, 11, and 12 show the wear of PCD insert at the end of experiment #5, 10, 14, and 15, respectively, for the three work specimens. The results show that excessive wear has been occurred for alloy-C and alloy-A than alloy-B at all the cutting conditions studied. The higher cutting forces, temperature, and vibrations caused the higher wear for the alloy-C and alloy-A. Wear mechanism is mostly dominant by the

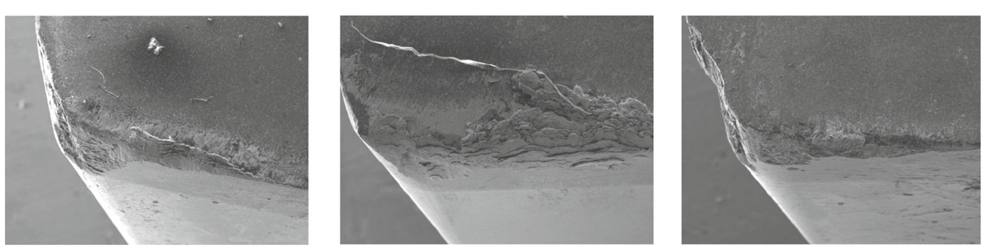

(a) wear of alloy-A (b) wear of alloy-B (c) wear of alloy-c

Fig. 11 Wear of PCD tool for three work specimens after test #14

(a) wear of alloy-A (b) wear of alloy-B (c) wear of alloy-c

Fig. 12 Removal of PCD insert from substrate for three work specimens after test #15

abrasion, chipping, and adhesion of the work material to the tool mainly due to increase in friction resulting in excessive heat generation and ultimately causing cutting tool wear.

Among the cutting conditions studied, it has been observed that wear of the PCD insert is most affected by the depth of cut as clear from Figs. 11 and 12. Removal of the PCD insert from the substrate has been observed for all three work specimens at experiment #15 ($a_p = 1.5$ mm) after an average of about 2.8 min of cut, which is mainly due to higher cutting forces, vibration amplitude, and higher temperature as well. EDAX analysis of the PCD insert near the worn cutting edge at rake face used in experiment #5, 10, and 14 has been carried out to study the adhesion of work material particles, and possible chemical reactions for all three work specimens and results are shown in Figs. 13, 14, and 15.

The EDAX analysis of worn inserts is carried out for analyzing the residual components on tool material which are resulted due to chemical reaction on the inserts with work material during cutting, and it reveals that more titanium particles are diffused into the PCD insert at higher cutting speed for alloy-A and alloy-C as compared to alloy-B. Moreover, this increase is more dominant for experiment #14, which shows that the effect of axial depth of cut is also more prominent in the adhesion of work material. This phenomenon usually occurs at temperature in excess of 500 °C [10] which shows that temperature at the tool-chip interface zone experienced temperature around this range for PCD insert. For alloy-B, which has a fine regular lamellar α + β Ti-6Al-4V microstructure, intensity of adhesion of work material is quite less showing that once a better microstructure is obtained after controlled heat treatment process, better results can be acquired for the machinability of titanium alloy Ti-6Al-4V with PCD tool and moderate increase in hardness can be compensated with superior properties of PCD tool.

Average flank wear (V_B) has been measured with ToupTek microscope software at the end of every experiment for the PCD inserts used for machining of the three work specimens, and results are plotted in Fig. 16.

Figure 16 shows the plots of tool wear at the end of each experiment, i.e., 300 s of cutting for all three specimens and about 168 s for experiment #15. It can be seen from the graphs above that tool wear is higher for alloys-A and C as compared to alloy-B which depicts that lower cutting forces, vibration, and temperature values helped in getting higher tool life for alloy-B at all the cutting conditions studied. The higher tool life for alloy-B is attributed to fine regular lamellar α + β Ti-6Al-4V structure achieved through controlled heat treatment. The tool wear is higher at higher cutting conditions especially when depth of cut is used in excess of 1.0 mm and feed rate above 0.1 mm/tooth. The tool wear is almost linear with the increase in cutting speed up to 150 m/min, but above this speed, a slight exponential trend is observed especially for alloy-C and alloy-A.

4 Conclusions

To analyze the effect of microstructure and hardness on the machinability of titanium alloy, Ti-6Al-4V with PCD tool has been evaluated in end-milling process. The cutting parameters, namely, cutting speed, axial depth of cut, and feed rate were varied; their effects have been studied on cutting forces, temperature, vibrations, and tool wear for two different heat-treated titanium alloys; and results are compared with titanium alloy in as-received condition. Results drawn for the study are summarized below:

1. PCD insert has shown improved performance when employed in machining of an alloy which was cooled in air after solution treatment followed by aging process as compared to other two specimens of titanium alloy Ti-6Al-4V. The main reason for better performance is attributed to formation of homogenous lamellar α + β Ti-6Al-4V structure due to a slow cooling rate of air. The increase in hardness of alloy-B as compared to alloy-A does not hinder its machinability because of superior properties of PCD tool as far as homogeneous microstructure is there.
2. Poor machinability was exhibited in all cutting conditions when PCD tool was employed in machining of alloy-C which was cooled in water after solution treatment followed by aging process. Formation of α′ martensite phase in its microstructure and the highest hardness after solution treatment and aging due to fast cooling rate of water are mainly attributed to such behavior of the alloy.
3. Results reveal that all the machinability evaluation parameters studied are strongly influenced by the axial depth of

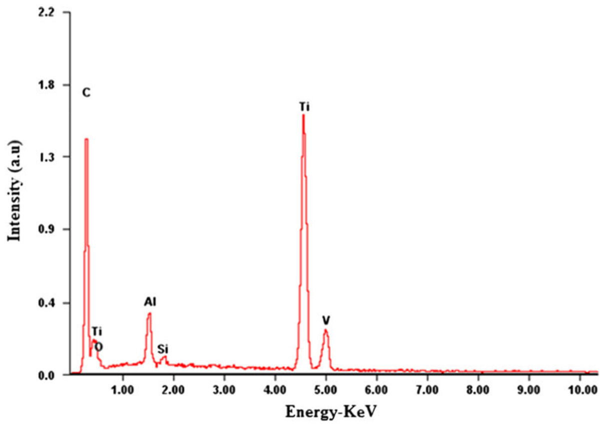

(a) Insert used in machining of alloy-A

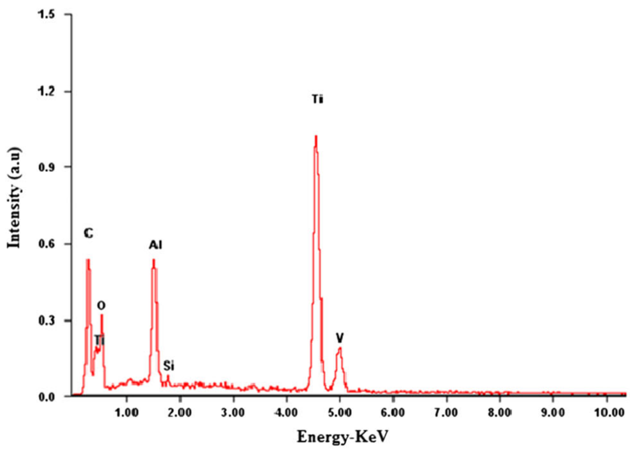

(b) Insert used in machining of alloy-B

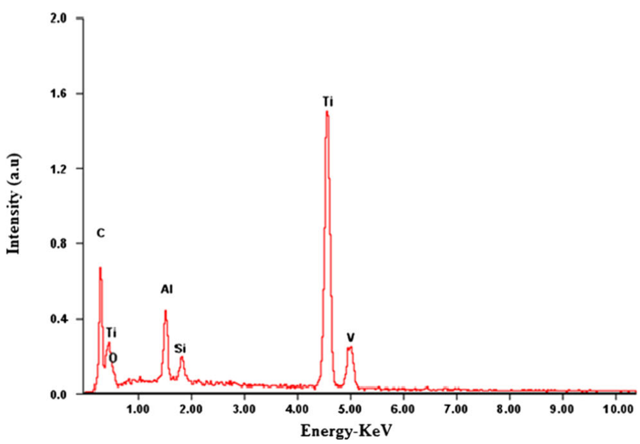

(c) Insert used in machining of alloy-C

Fig. 13 EDAX analysis of PCD tool for three work specimens after test #05

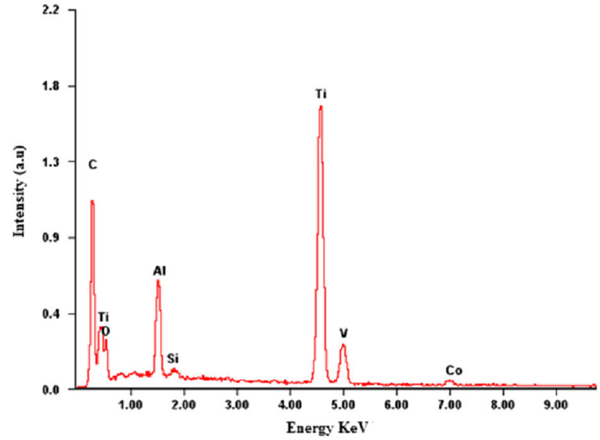

(a) Insert used in machining of alloy-A

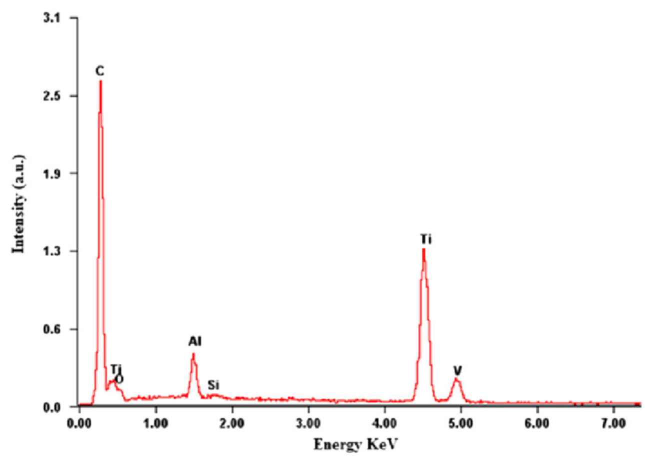

(b) Insert used in machining of alloy-B

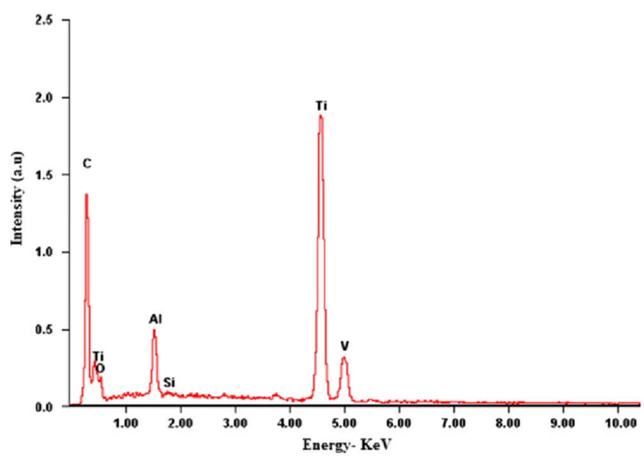

(c) Insert used in machining of alloy-C

Fig. 14 EDAX analysis of PCD tool for three work specimens after test #10

cut and feed rate. While cutting speed has slight or moderate effect up to speed of about 170 m/min, when cutting speed used in excess of 200 m/min and combined with a higher feed rate and depth of cut, all the evaluation parameters increase with a slightly higher ratio with more increase for alloy-A and alloy-C. The higher influence of axial depth of cut and feed rate is further confirmed when PCD insert was removed from the substrate for all three

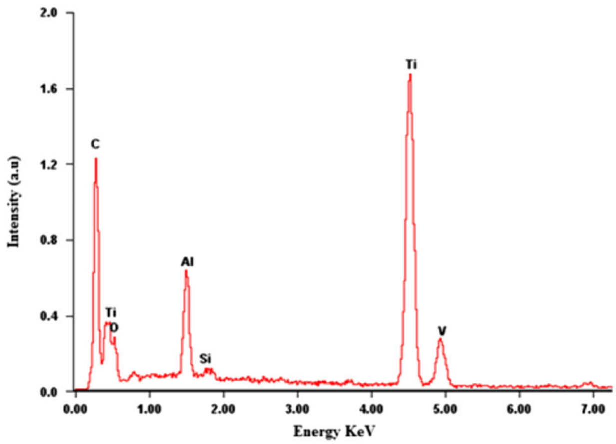

(a) Insert used in machining of alloy-A

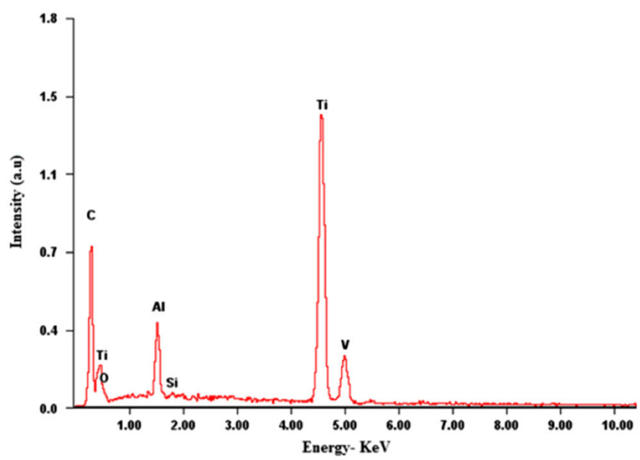

(b) Insert used in machining of alloy-B

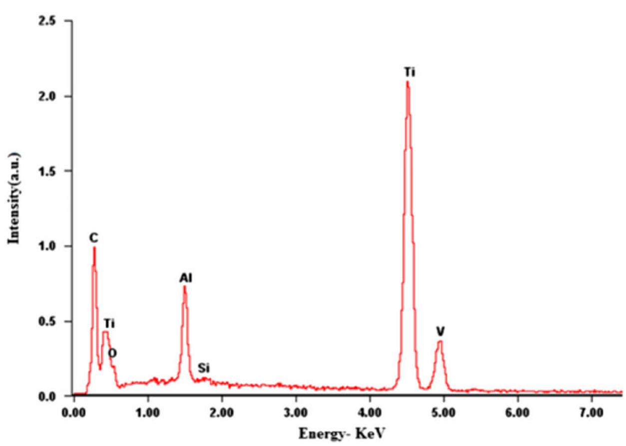

(c) Insert used in machining of alloy-c

Fig. 15 EDAX analysis of PCD tool for three work specimens after test #14

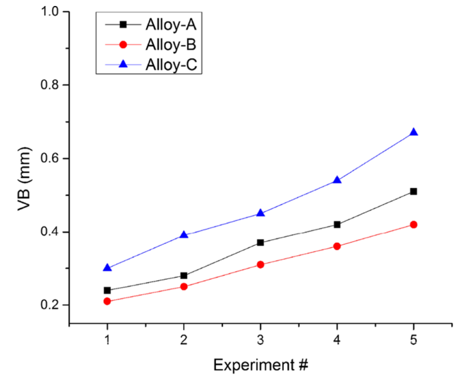

(a) Effect of cutting speed, V_C

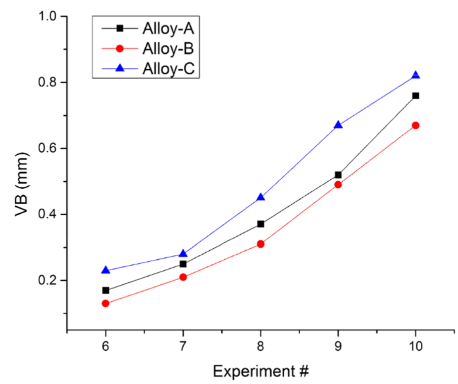

(b) Effect of feed per tooth, f_Z

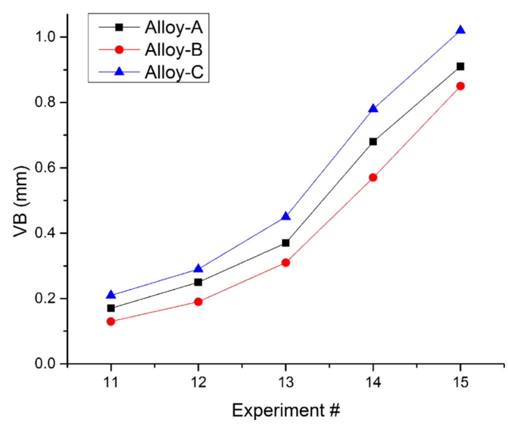

(c) effect of axial depth of cut, a_P

Fig. 16 Max. wear land (VB) of PCD insert at the end of experiments for all three specimens

alloys when axial depth of cut was used in the excess of 1.5 mm, feed of 0.1 mm/tooth, and cutting speed of 150 m/min. The forces and the vibrations have the highest values at this cutting condition as well.

4. From the results, it can be concluded that machinability of titanium alloy Ti-6Al-4V can be further improved with PCD tools with controlled heat treatment process as explored in this study. An improvement of about 10 to 20 % has been observed in terms of tool life and productivity by increasing the cutting speed on the homogeneous microstructure Ti-6Al-4V heat-treated alloy.

Acknowledgments The authors are grateful for the financial support provided by the Key National Science and Technology Project of China (grant no. 2013ZX04001-011) and the State Key Laboratory of Tribology Foundation of China (grant no. SKLT2013B03) in execution of this research work, and they are also thankful to all the technicians and lab engineers who provided their help and technical support for the accomplishment of all the experimental and analysis work.

References

1. Armendia M, Garay A, Iriarte L-M, Arrazola P-J (2010) Comparison of the machinabilities of Ti6Al4V and TIMETAL® 54M using uncoated WC–Co tools. J Mater Process Technol 210(2):197–203
2. Rahman M, Wong YS, Zareena AR (2003) Machinability of titanium alloys. JSME Int J Ser C 46:17–115
3. Ezugwu EO, Bonney J, Yamane Y (2003) An overview of the machinability of aero engine alloys. J Mater Process Technol 133:233–253
4. Li L, Chang H, Wang M, Zuo DW, He L (2004) Temperature measurement in high speed milling Ti6Al4V. Key Eng Mater. 259–260: 804–808
5. Jawaid A, Sharif S, Koksal S (2000) Evaluation of wear mechanisms of coated carbide tools when face milling. J Mater Process Technol 99:266–274
6. Wang ZG, Rahman M, Wang YS (2005) Tool wear characteristics of binderless CBN tools used in high speed milling of titanium alloys. Wear 258:752–758
7. Kuljanic E, Fioretti M, Beltrame L, Miani F (1998) Milling titanium compressor blades with PCD cutters. CIRP Ann Manuf Technol 47(1):61–64
8. Nabhani F (2001) Machining of aerospace titanium alloys. Robot Comput Integr Manuf 17(1–2):99–106
9. Amin AKMN, Ismail Ahmad F, Khairusshima MK (2007) Nor, effectiveness of un-coated WC-Co and PCD inserts in end milling of titanium alloy – Ti6Al4V. J Mater Process Technol. 192–193: 147–158
10. Pan W, Ding S, Mo J (2014) Thermal characteristics in milling Ti6Al4V with polycrystalline diamonds tools. Int J Adv Manuf Technol 75:1077–1087
11. Ezugwu EO, Bonney J, Rosemar B, Silva D, Cakir O (2007) Surface integrity of finished turned Ti-6Al-4V alloy with PCD tools using conventional and higher pressure coolant supplies. Int J Mach Tool Manuf 47:884–891
12. Konig W, Neises N (1993) Turning TiAl6V4 with PCD. Ind Diamond Rev 53(1):85–88
13. Honghua SU, Peng L, Yucan FU, Jiuhua XU (2012) Tool life and surface integrity in high-speed milling of titanium alloy TA15 with PCD/PCBN tools. Chin J Aeronaut 25:784–790
14. Kosaka Y, Fox SP (2004) Influence of alloy chemistry and microstructure on the machinability of titanium alloys. In Proceedings of Cost Affordable Titanium TMS Conference, 169–176
15. Kosaka Y, Fanning JC, Fox SP (2004) Development of low cost high strength alpha/beta alloys with superior machinability. In Proceedings of 10th world conference on titanium. 3028–3034
16. Khanna N, Garay A, Iriarte LM, Soler D, Sangwan KS, Pedro J (2012) Arrazola, effect of heat treatment conditions on machinability of Ti64 and Ti54M alloys. In Proceedings of 5th CIRP Conference on High Performance Cutting, Procedia CIRP 1: 477–482
17. Khanna N, Sangwan KS (2013) Machinability study of α/β and β titanium alloys in different heat treatment conditions. Proc IMechE Part B: J Eng Manuf 227(3):357–361
18. Rahim EA, Sharif S (2006) Investigation on tool life and surface integrity when drilling Ti-6Al-4V and Ti-5Al-4V-Mo/Fe. J Soc Mech Eng Int J 49:340–345
19. Venkatesh V, Kosaka Y, Fanning J, Nyakana S (2007) Processing and properties of Timetal 54M. In Proceedings of 11th world conference on Titanium, Kyoto, Japan, 713–716
20. Armendia M, Garay A, Iriarte LM, Belloso J, Turner SM, Osborne P, Arrazola PJ (2010) The influence of heat treatment in the machinability of titanium alloys: Ti6Al4V and Ti-5Al-4V-0.6Mo-0.4Fe (Ti54M). In Proceedings of 4th CIRP International Conference on High Performance Cutting, Japan, C02
21. Azam M, Jahanzaib M, Wasim A, Hussain S (2015) Surface roughness modeling using RSM for HSLA steel by coated carbide tools. Int J Adv Manuf Technol 78:1031–1041
22. Pinke P, Žitňanský, Čaplovič L', Réger M (2004) The influence of heat treatment parameters on the microstructure of Ti6Al4V titanium alloy. In Proceedings of International Scientific Conference COMAT-TECH, Bratisalva: Vydavatel, STU. 1042–1046
23. Anayet UPM, Amin AKMN, Faris WF (2009) Prediction of tangential cutting force in end milling of medium carbon steel by coupling design of experiments and response surface methodology. J Mech Eng 40:2
24. Amin AKMN, Talantov NV (1986) Influence of the instability of chip formation and preheating of work on tool life in machining high temperature resistant steel and titanium alloys. Mech Eng Residuals Bull 9:52–62
25. Komanduri R, Hou ZB (2002) On the thermoplastic shear instability in the machining of a titanium alloy (Ti-6Al-4V). Metall Mater Trans A 33:2995–3010